LAWRENCE
LIVERMORE
NATIONAL
LABORATORY

LLNL-JRNL-741079

A survey of conductive and plasmonic materials for high power optical applications

J. H. Yoo, S. Rafique, S. Falabella, H. Zhao, S. Elhadj

November 2, 2017

Physica Status Solidi (a) # applications and materials science

Disclaimer

WILEY-VCH

LLNL-JRNL-741079

A Survey of Transparent Conducting Films and Opto-Electrical Materials for High Optical Power Applications

*Jae-Hyuck Yoo, Andrew Lange, John Chesser, Steve Falabella, and Selim Elhadj**

Dr. J.-H. Yoo, Dr. A. Lange
Physical and Life Sciences Directorate, Lawrence Livermore National Laboratory, Livermore, CA 94550, USA

J. Chesser, S. Falabella, Dr. S. Elhadj
Engineering Directorate, Materials Engineering Division, Lawrence Livermore National Laboratory, Livermore, CA 94550, USA
E-mail: elhadj2@llnl.gov

Keywords: Laser damage, transparent conducting films, plasmonic materials

The lifetime laser damage performance of a wide range of transparent conductive materials is assessed, including ultrathin metal films, doped metal oxides, doped compound semiconductors, and graphene whose carrier densities span 5 orders of magnitude from 10^{18} to 10^{23} cm^{-3}. Lifetime laser damage thresholds were determined by exposing material surfaces to repeated nanosecond laser pulses at near infrared wavelenghts (1064 nm). Near threshold fluences, two distinct damage modes, i.e. bulk and discrete, emerge depending on carrier density. These bulk and discrete damage modes are attributed to free carrier-induced bulk and localized, defect-driven absorption processes, respectively. For polycrystalline films with free carrier densities greater than ~10^{20} cm^{-3}, laser damage thresholds are less than 5 J/cm^2. In contrast, bulk absorption is not apparent at thresholds substantially higher than ~10 J/cm^2 in single crystal films with free carrier concentrations lower than ~10^{19} cm^{-3}. By increasing thickness, films with lower carrier densities can deliver relevant levels of sheet conductance (< 200 Ω/sq) while remaining transparent. These lifetime laser damage threshold measurements offer a systematic criteria to select materials aimed at handling high optical powers in optoelectronics devices and emerging plasmonic and metamaterials for lasers.

1. Introduction

Conductive materials with high free-carrier concentrations are critical components in optoelectronic devices. When deposited as films or fabricated into nanostructures, they can be used as optically transparent electrodes, semimetals for dynamic beam modulation devices,[1, 2] or plasmonic sensors.[3] However, for these applications, heat generated from electron-phonon coupling[4] imposes performance limitations, especially for applications that require high optical power handling for which excessive heat can lead to catastrophic damage or, under repeated exposures, to fatige and degradation. In order to reduce thermally-induced damage, the heat generation must be minimized. Recently, thermal management strategies for the improvement of laser damage performance in tin-doped indium oxide (ITO) transparent conducting films (TCFs) have been demonstrated.[5] These so-called thermal ruggedization strategies for handling high energy short laser pulses focus on maximizing heat dissipation by using substrates with high thermal conductivity and adding transparent capping layers to act as heatsinks. Another ruggedization strategy is to minimize the coefficient of light absorption (α) in ITO films by reducing their free carrier concentrations (N_e) and increasing their electron mobilities (μ_e) since α is directly related to N_e and $1/\mu_e$. This minimization of α also reduces parasitic optical losses (ε_2) in plasmonic materials, which represents the imaginary part of the permittivity (ε_2) as expressed by $2nk = 2n(\alpha\lambda/4\pi)$, where n is the real part and k is the imaginary part of refractive index, respectively.[6]

One thin film materials optimization strategy for laser applications involves adjusting the optical and electronic properties, while concurrently improving their laser damage performance. However, as the discussion above implies, these requirements can be mutually exclusive depending on the required sheet conductance and laser wavelength to be addressed. Thus, there is a need to identify materials that can withstand the optical fluences of modern

high repetition rate laser systems with high average and high peak power, while maintaining high conductance. Conductive films that are transparent to near infrared (NIR) wavelengths are particularly important because of the ubiquitious use of Nd:YAG lasers with a fundamental emission wavelength of 1064 nm[7-9]; TCFs that are functional at this wavelength can also support plasmonic coupling from intraband transitions.[10] To that end, this study surveys the lifetime laser damage threshold of a range of transparent and conductive materials with N_e spanning five orders of magnitude from 10^{18} to 10^{23} cm^{-3}, sheet resistances < 200 Ω/sq, and total transmission at 1064 nm ranging from 30 to 85%. These parameters (i.e. damage threshold, N_e, sheet resistance, and damage mode) may guide material selection for specific device applications by use of appropriate figure of merit, but this time also accounting for laser damage thresholds.[11, 12] Measurements of laser lifetime damage thresholds (fluence at onset of damage that becomes apparent under optical microscope), F_{th}, is performed using short-pulse nanosecond exposures on single crystal films including silicon-doped gallium nitride (GaN), silicon-doped β-gallium oxide (Ga_2O_3), tin-doped β-Ga_2O_3, and nitrogen-doped 6H-silicon carbide (SiC), as well as polycrystalline films including graphene, ultrathin gold (Au), ITO, fluorine-doped tin oxide (FTO), aluminum-doped zinc oxide (AZO), and titanium nitride (TiN). Lifetime thresholds of these materials are then related to their opto-electrical properties to explore the dominant failure mechanisms and operating windows. This study can thus serve as a material selection guide for transparent electrodes and plasmonic materials for optoelectronic devices where low losses and peak lifetime performance are critical.

2. Results and discussion

The multi-pulse F_{th} measurements are based on two equivalent laser damage testing methods. The first derives laser damage probability curves for N number of shots as described elsewhere[13], which is especially well-suited to address materials exhibiting a stochastic laser

damage behavior with respect to the laser fluence energy applied. The second, validated recently, uses the more efficient laser damage size analysis (DSA) method that is especially well-suited to produce large datasets involving a high number of multiple pulse exposures, samples with limited areas to test, and for materials exhibiting more deterministic fluence-dependent laser damage.[14-16] The laser setup for this material study consists of a NIR (1064 nm) Nd:YAG laser, with pulse length of 7 ns, and a repetition rate of 10 Hz. A detailed description of the laser damage system can be found in a previous report.[17] The film thicknesses are measured at mask or ablation step edges using a confocal laser microscope (Keyence, VK-X100). Except for the TiN sample that was deposited on a conductive p-doped silicon substrate, the sheet resistance, mobility, and carrier concentration were measured for all films using a Hall effect measurement system (Ecopia, HMS-3000) with the measured film thickness as a fixed input. The electrical properties of the TiN sample were measured using ellipsometry data fit to a Drude dispersion model.[18] The material properties measured in this study are summarized in **Table 1**. In that group, only GaN, SiC, and β-Ga_2O_3 are single crystalline (films or bulk), the other materials including oxides, graphene, and gold are all polycrystalline as determined by XRD measurements (data not shown).

Single shot (N=1) damage morphologies were initially determined for single crystal and polycrystalline materials near their damage thresholds to probe differences in their damage processes (**Figure 1**). The resulting dominant damage modes reveal a sharp difference between high free carrier ($N_e > 10^{20}$ cm^{-3}), polycrystalline materials that fail by apparent bulk absorption, and single crystal materials with $N_e < 10^{19}$ cm^{-3} that fail by apparent localized defect-driven absorption processes. For polycrystalline materials, the ablative and darkening damage is very deterministic and tracks the shape of the round Gaussian beam consistent with a bulk absorption process forming a gross distributed damage morphology. In contrast, the lower N_e single crystal materials damaged as localized eruption events producing pits much

smaller than the beam size and at nearly random locations with respect to the beam fluence map. Still, as previoulsy reported, the laser absorption that initiates film damage is mostly confined to photoluminescent defect-rich regions located at or near film interfaces and free surfaces.[19, 20] Delocalized, bulk damage where free carrier absorption is the dominant absorption process is apparent in all polycrystalline film tested ($N_e > 10^{20}$ cm^{-3}). The damage mode then switches to a much smaller localized absorption process for single crystal materials with $< N_e \sim 10^{19}$ cm^{-3} using the same beam size, even for exposures with higher pulse fluences than those used on polycrystalline films. This result is consistent with previous results on ITO, where polycrystalline films with intentionally lowered N_e was made to damage via a localized, defect-driven damage mode, whereas polycrystalline ITO films with higher N_e damaged via bulk damage processes.

The multi-pulse ($N \leq 1000$) laser damage thresholds are shown in **Figure 2** for all materials that were tested for lifetime assessment using the DSA laser damage method,[15] which included all polycrystalline materials with high bulk absorption and $N_e > 10^{20}$ cm^{-3} (Table 1). Amongst these samples, graphene and gold ultrathin films on fused silica (Au/F) showed relatively low lifetime damage thresholds $F_{th} \sim 0.25$ J/cm^2. The substrate played an important role in affecting the damage threshold from laser induced heating. The gold on sapphire sample (Au/S) has twice the threshold of the gold on glass (a poor thermal conductor) sample with the same gold film thickness. This result is consistent with previous experimental results on ITO, and further confirmed by laser induced heating simulations of ITO showing larger temperature excursions of an ITO film on a fused silica substrate compared to the temperature of the same ITO film on a sapphire substrate.[5] Amongst the ITO, FTO, and AZO metal oxide samples (all on the same glass substrates), the thickest AZO film had the highest threshold, which is likely related to this AZO sample having the lowest N_e in that group. Laser incubation, whereby the damage threshold, $F_{th}(N)$, decreases with the number of exposures

N,[17] occurred for all samples tested in Figure 1, including the single crystal materials. The damage thresholds tended to stabilize at ~50±10% of the single pulse threshold for all materials for N larger than > ~100, suggesting that these materials could operate below these fluence thresholds. The incubation behavior is due to material fatigue and/or increased absorption rapidly leading to catastrophic failure as reported previously for ITO.[17] The dashed lines in Figure 2 are based on an empirical fatigue model, $F_{th}(N) = F_{th}(\infty) + [F_{th}(1) - F_{th}(\infty)] \exp[-k(N-1)]$, where k is an incubation factor, which is related to how quickly the threshold deteriorates with N.[21] The least-square fitted parameters ($F_{th}(1)$, $F_{th}(\infty)$, and k) are included in the plot of Figure 2 and relate to how optically robust each material is when subjected to repeated laser shots. Graphene and AZO are at the extreme of the range of threshold fluences for the polycrystalline materials, with the AZO film being the most robust while still maintaining overall good conductance due to its large cross sectional thickness available for charge transport (Table 1).

To address the lifetime damage thresholds of all materials in this study, including the single crystal materials, the dependence of laser damage probability on fluence was determined for all materials for comparison. The $F_{th}(N = 100)$ threshold values were determined to provide a good measure of lifetime performance values since the threshold fluences appear to plateau for N > ~100 (Figure 2), as was previously observed in the lifetime damage threshold of GaN films.[20] Indeed, the position of the probability curves for SiC, Ga_2O_3, and GaN for N = 1, 10, 100, and 1000 overlapped as the number of pulse shot reached 100 for these single crystal materials (data not shown). The laser damage probabilities data curves are shown in **Figure 3**, except for TiN for which the lifetime threshold was determined using the DSA laser damage test method due to the limited test area available on that sample. Lifetime damage thresholds (for N = 100), correspond to the fluence points where the fitted probability curves begin to rise (i.e, at the onset of damage), which are reported along with the curves presented as two separate panels for clarity (Figure 3(a) and 3(b)). The fluence, F,

dependent probability curves, *P(F)*, are based on Poisson statistics given by $P(F) = 1 - \exp[-N(F)]$, where the number, *N(F)*, represents a number areal density of active damage precursors.[22]

The lifetime thresholds are replotted in **Figure 4(a)** for direct comparison of the materials measured lifetime threshold values on a log scale. Two class of material systems emerge when focusing on these laser damage performance results. First, the polycrystalline materials such as the metal oxides, which tend to require a high free carrier density above ~10^{20} cm^{-3} to overcome grain boundary (GB) transport energy barriers, Φ_B, related to GB trap states.[23] The charge transport barriers scales exponentially with $-\Phi_B/kT \propto 1/N_D$ where, N_D is the number of charge carrier donor states. Thus, polycrystalline systems absorption and damage will tend to be dominated by free carrier concentration limiting their laser damage lifetime thresholds (Figure 4(a)). Second, for single crystal systems such as low-doped GaN, the N_e and thus free carrier absorption can be lowered by order of magnitudes, while still advantageously increasing carrier mobility from lowered impurity dopant scattering. In contrast, carrier mobility in polycrystalline materials requires a higher level of doping to reduce the activation energy involved in charge transport across grain boundaries.[24] Still, sparse extrinsic localized defects, especially in heteroepitaxially grown materials, will limit single crystal damage performance but at higher lifetime threshold fluences compared to the polycrystalline materials as illustrated in Figure 4(a). Therefore, single crystal materials with lower free carrier concentrations are in principle ideal for high damage performance transparent electrodes applications. Generally, however, carrier concentrations in single crystals may not exceed ~10^{19} cm^{-3} due to stress from introduction of dopants in the crystal lattice,[25] extending their use in the mid- to far infrared wavelenghts (i.e. near their plasma frequency). Within the group of polycrystalline materials those with the lowest N_e (Figure 4(b)) had the

highest damage thresholds as expected, except for graphene, which has significant optical absorbance due to interband transitions in the NIR.[26] It has been shown that polycrystalline In_2O_3 and SnO_3 films doped with transition metals can have high mobilities, ~100 cm^2/Vs, thereby easily producing low sheet resistances (< 100 Ω/sq) with relatively low carrier concentrations (< 10^{20} cm^{-3}).[28-32] These high mobility oxide materials may therefore be suitable candidates for high optical power applications with the added benefits of lower cost and scalability relative to single crystal films. Of interest, is the results on TiN (N_e = 10^{22} cm^{-3}), which despite having ~ 10×N_e of ITO, had a comparable damage performance in the NIR and a higher damage performance than the plasmonic reference gold ultrathin film likely due to TiN "refractory" nature.[27] Sheet resistance, R_s, which is related to N_e, μ_e, and film thickness by $R_s \propto 1/(\mu e N_e t)$ can be adjusted by controlling the thickness and mobility for a given N_e to maintain conductance (Table 1), although for polycrystalline materials the N_e must typically be > 10^{19}-10^{18} cm^{-3} to achieve reasonable levels of conduction.

All the films used in this study had R_s < 200 Ω/sq (Figure 4(c)) making them relevant to fast switching or large aperture optoelectronic applications. A strong correlation of damage threshold with the absorption coefficient is apparent in Figure 4(d), since the extent of heating in the short pulse regime is determined by the energy density absorbed when heat diffusion is limited by short pulse exposures.

3. Conclusions

In general, we establish here a direct relation between lower laser damage lifetime thresholds of transparent opto-electrical materials with high free carrier absorption when subjected to high peak power exposures. Thus thicker transparent films of single crystal wide bandgap semiconductors with low carrier densities < 10^{19} cm^{-3} appear to be ideal for handling high power levels while still maintaining conductance. In contrast, polycrystalline films that

require higher levels of doping for charge transport across grain boundaries will have higher levels of laser energy absorption, fundamentally limiting their use in high power applications. Suitability for future applications that could consider the class of materials surveyed here may include large area, high power handling actively addressed devices designed for fast switching or for steering high average or high peak power lasers, or the development of low loss metamaterials capable of handling laser energetics. Other technologies involving transparent conductive films may also account for material cost or scalability based on a suitable figure of merit for selection, which is now extended to account for the lifetime laser damage fluence threshold material properties presented in this study.

4. Experimental section

Absorption coefficient calculation: For transparent samples (e.g., Graphene, ITO, FTO, AZO, β-Ga_2O_3 film, GaN, SiC bulk, and β-Ga_2O_3 bulk), reflectance (R) and transmittance (T) at 1064 nm with zero angle of incidence were measured using a customized transmission/reflectance optical measurement setup. Absorptance (A) was then calculated using the relationship $A = 1 - R - T$ with the assumption that scattering was negligible. For each sample, film thickness (t) was measured and the absorption coefficient (α) was calculated using $A = \exp(-\alpha t)$ by the Beer's law. A spectroscopic ellipsometer (J. A. Woollam) was used to estimate the optical properties of opaque samples (e.g., Au/F, Au/S, and TiN) using the Drude model. This estimation was validated by measuring the film thicknesses.

Damage size analysis (DSA) method: The damage size analysis (DSA) method is described in detail.[15] Briefly, for deterministic laser damage induced by a Gaussian shaped laser beam, the boundary of a damage site ($R_{boundary}$) is formed where the beam fluence is equal to the laser damage threshold. Therefore, under laser irradiation at a known peak laser fluence

(F_{peak}) and 1/e^2 laser beam radius (w_o), laser damage morphology provides laser damage threshold (F_{th}) information by $F_{th} = F_{peak}$ exp (-2 ($R_{boundary}/w_o$)^2).

Acknowledgements

This work performed under the auspices of the U.S. Department of Energy by Lawrence Livermore National Laboratory under contract DE-AC52-07NA27344 within the LDRD program. Project 15-ERD-057 was funded by the LDRD Program at LLNL. We thank S. Rafique and H. Zhao for providing CVD Ga_2O_3 samples used in this study.

Received: ((will be filled in by the editorial staff))
Revised: ((will be filled in by the editorial staff))
Published online: ((will be filled in by the editorial staff))

References

[1] E. Feigenbaum, K. Diest, H. A. Atwater, *Nano Lett.* **2010**, *10*, 2111.
[2] G. K. Shirmanesh, R. Sokhoyan, R. A. Pala, H. A. Atwater, *Nano Lett.* **2018**, *18*, 2957.
[3] M. E. Stewart, C. R. Anderton, L. B. Thompson, J. Maria, S. K. Gray, J. A. Rogers, R. G. Nuzzo, *Chem. Rev.* **2008**, *108*, 494.
[4] M. Xu, J. Y. Yang, S. Y. Zhang, L. H. Liu, *Phys. Rev. B* **2017**, *96*, 115154.
[5] J. H. Yoo, M. Matthews, P. Ramsey, A. C. Barrios, A. Carter, A. Lange, J. Bude, S. Elhadj, *Opt. Express* **2017**, *25*, 25533.
[6] P. R. West, S. Ishii, G. V. Naik, N. K. Emani, V. M. Shalaev, A. Boltasseva, *Laser Photonics Rev.* **2010**, *4*, 795.
[7] W. T. Pawlewicz, R. Busch, *Thin Solid Films* **1979**, *63*, 251.
[8] J. Heebner, M. Borden, P. Miller, C. Stolz, T. Suratwala, P. Wegner, M. Hermann, M. Henesian, C. Haynam, S. Hunter, K. Christensen, N. Wong, L. Seppala, G. Brunton, E. Tse, A. Awwal, M. Franks, E. Marley, K. Williams, M. Scanlan, T. Budge, M. Monticelli, D. Walmer, S. Dixit, C. Widmayer, J. Wolfe, J. Bude, K. McCarty, J. M. DiNicola, *P. Soc. Photo-Opt. Ins.* **2010**, *7842*, 78421C.
[9] M. J. Matthews, G. Guss, D. R. Drachenberg, J. A. Demuth, J. E. Heebner, E. B. Duoss, J. D. Kuntz, C. M. Spadaccini, *Optics Express* **2017**, *25*, 11788.
[10] M. R. Beversluis, A. Bouhelier, L. Novotny, *Phys. Rev. B* **2003**, *68*, 115433.
[11] G. Haacke, *J. Appl. Phys.* **1976**, *47*, 4086.
[12] D. S. Ghosh, T. L. Chen, V. Pruneri, *Appl. Phys. Lett.* **2010**, *96*, 041109.
[13] H. Krol, L. Gallais, C. Grezes-Besset, J. Y. Natoli, M. Commandre, *Opt. Comm.* **2005**, *256*, 184.
[14] M. Sozet, J. Neauport, E. Lavastre, N. Roquin, L. Gallais, L. Lamaignere, *Opt. Lett.* **2016**, *41*, 804.
[15] S. Elhadj, J. H. Yoo, *Opt. Lett.* **2017**, *42*, 3153.
[16] Y. F. Hao, M. Y. Sun, Z. Y. Jiao, Y. J. Guo, X. Pan, X. Y. Pang, J. Q. Zhu, *Appl. Optics* **2018**, *57*, 4191.
[17] J. H. Yoo, A. Lange, J. Bude, S. Elhadj, *Opt. Mater.* Express **2017**, *7*, 817.
[18] S. D'Elia, N. Scaramuzza, F. Ciuchi, C. Versace, G. Strangi, R. Bartolino, *Appl. Surf. Sci.* **2009**, *255*, 7203.

[19] J. H. Yoo, M. G. Menor, J. J. Adams, R. N. Raman, J. R. I. Lee, T. Y. Olson, N. Shen, J. Suh, S. G. Demos, J. Bude, S. Elhadj, *Optics Express* **2016**, *24*, 17616.
[20] S. Elhadj, J. H. Yoo, R. A. Negres, M. G. Menor, J. J. Adams, N. Shen, D. A. Cross, I. L. Bass, J. D. Bude, *Opt. Mater. Express* **2017**, *7*, 202.
[21] A. Rosenfeld, M. Lorenz, R. Stoian, D. Ashkenasi, *Appl. Phys. A-Mater.* **1999**, *69*, S373.
[22] R. H. Picard, D. Milam, R. A. Bradbury, *Appl. Optics* **1977**, *16*, 1563.
[23] T. Tsurumi, S. Nishizawa, N. Ohashi, T. Ohgaki, *Jpn. J. Appl. Phys.* 1 **1999**, *38*, 3682.
[24] M. Roschke, F. Schwierz, *IEEE T. Electron Dev.* **2001**, *48*, 1442.
[25] L. T. Romano, C. G. Van de Walle, J. W. Ager, W. Gotz, R. S. Kern, *J. Appl. Phys.* **2000**, *87*, 7745.
[26] K. F. Mak, L. Ju, F. Wang, T. F. Heinz, *Solid State Comm.* **2012**, *152*, 1341.
[27] U. Guler, A. Boltasseva, V. M. Shalaev, *Science* **2014**, *344*, 263.
[28] S. Calnan, A. N. Tiwari, *Thin Solid Films* **2010**, *518*, 1839
[29] D. S. Bhachu, D. O. Scanlon, G. Sankar, T. D. Veal, R. G. Egdell, G. Cibin, A. J. Dent, C. E. Knapp, C. J. Carmalt, I. P. Parkin, *Chem. Mater.* **2015**, *27*, 2788.
[30] N. Yamada, M. Yamada, H. Toyama, R. Ino, X. Cao, Y. Yamaguchi, Y. Ninomiya, *Thin Solid Films* **2017**, *626*, 46.
[31] S. Nakao, N. Yamada, T. Hitosugi, Y. Hirose, T. Shimada, T. Hasegawa, *Appl. Phys. Express* **2010**, *3*, 31102.
[32] K. Iketaki, T. Kaji, S. Nakao, M. Hiramoto, *Phys. Status Solidi C* **2011**, *8*, 543.
[33] S. Rafique, L. Han, A. T. Neal, S. Mou, M. J. Tadjer, R. H. French, H. P. Zhao, *Appl. Phys. Lett.* **2016**, *109*, 132103.

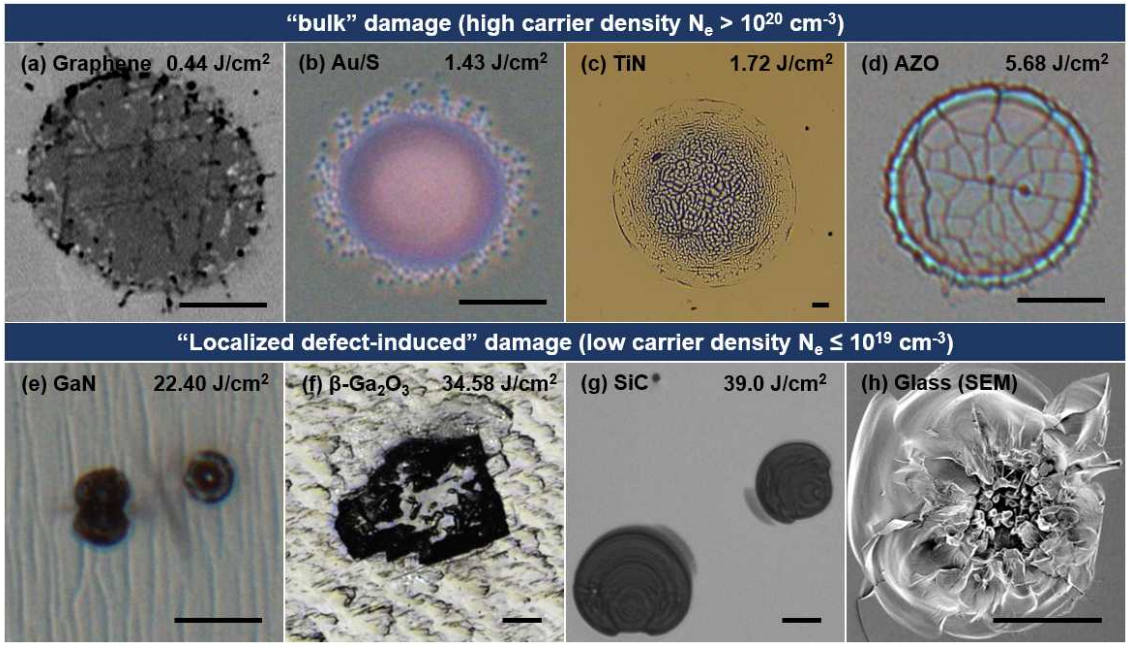

Figure 1. Damage morphology of single-pulse laser damage test sites. (a) Graphene, (b) Gold film on sapphire (Au/S), (c) Titanium nitride (TiN), (d) Aluminum-doped zinc oxide (AZO), (e) Gallium nitride (GaN) film, (f) Silicon-doped β-gallium oxide (Ga_2O_3) film, (g) Nitrogen-doped silicon carbide (SiC) bulk, and (h) fused silica bulk. The scale bars are 20 μm.

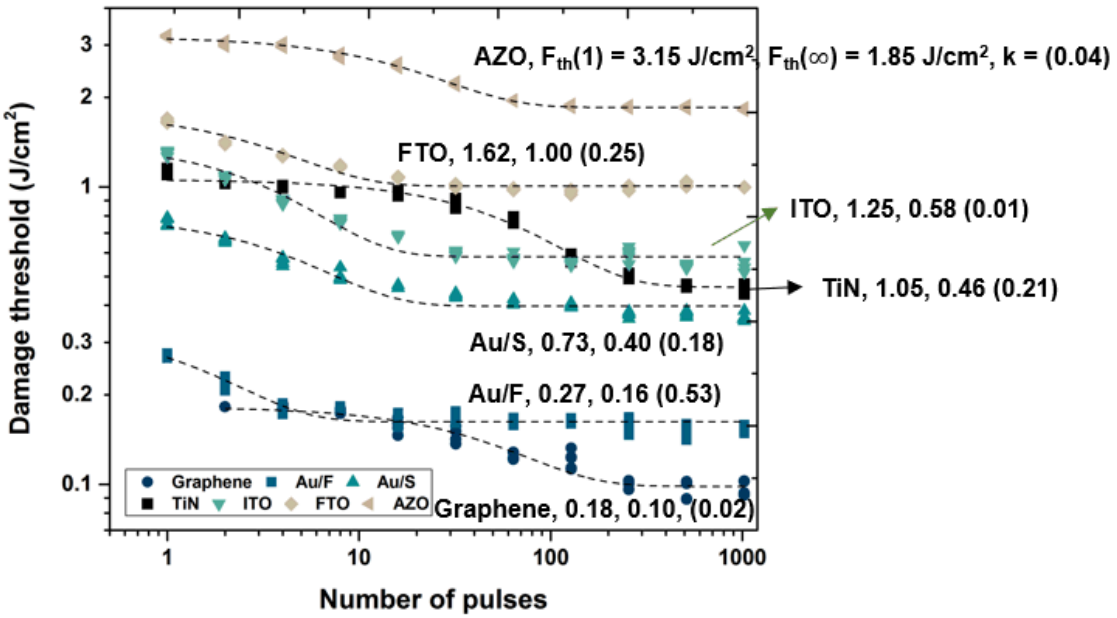

Figure 2. Measured multi-pulse (lifetime) laser damage thresholds shown on a log-log scale. Threshold values were derived using DSA laser damage testing method.

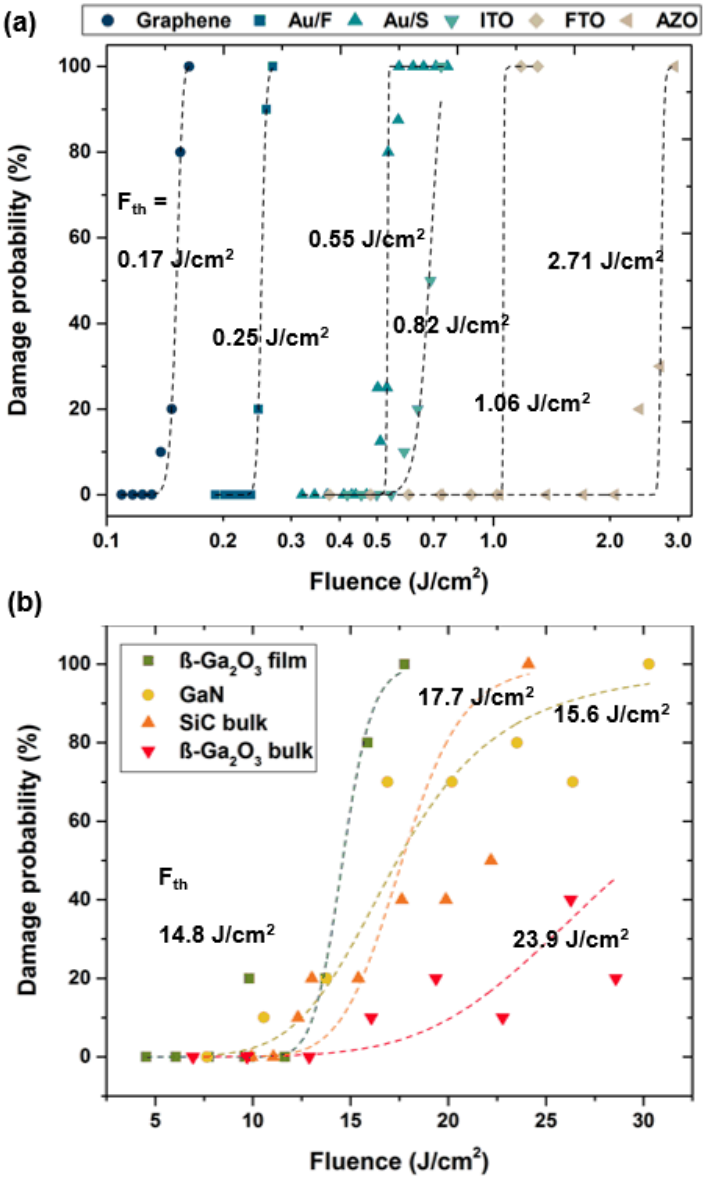

Figure 3. Damage probability curves of (a) the bulk damage sample group on a semi-log scale and (b) the discrete damage sample group on a linear scale.

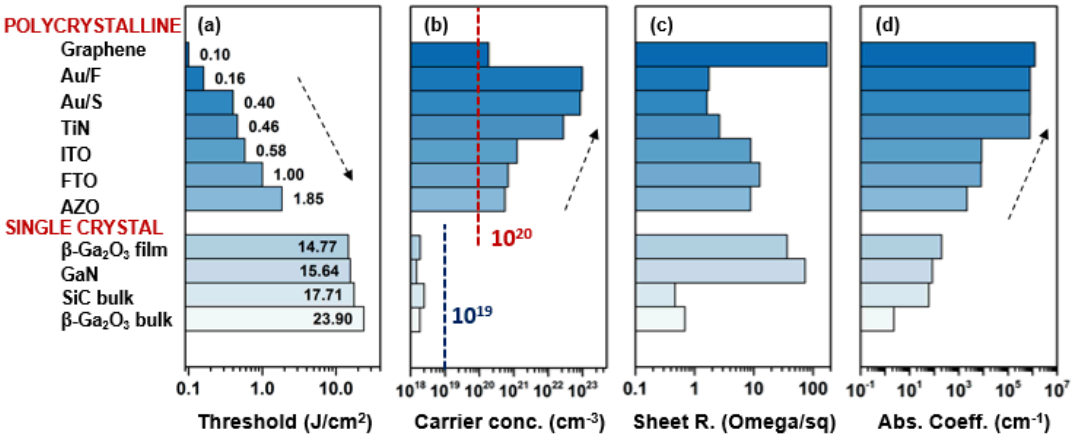

Figure 4. (a) Lifetime laser damage performance, (b) carrier concentration, (c) resistivity, and (d) absorption coefficient for a range of transparent conducting materials.

Table 1. Physical, electrical, and optical properties of samples.

Type	Name	Substrate	Deposition/growth method [Supplier]	Thickness [nm]	Sheet resistance [Ω/□]	Mobility [cm^2/Vs]	Carrier concentration [#/cm^3]
Poly crystalline	Graphene[a)]	Fused silica	Single layer graphene (SLG) [ACS Materials]	~1	175	1920	1.86×10^{13} [b)]
	Au/F	Fused silica	E-beam evaporation [AC-VPL, LLNL]	25.9	1.74	14.1	9.81×10^{22}
	Au/S	Sapphire	E-beam evaporation [AC-VPL, LLNL]	25.1	1.63	17.8	8.57×10^{22}
	TiN	Silicon	Cathodic arc deposition [AC-VPL, LLNL]	344	2.64[c)]	2.49[c)]	2.76×10^{22} [c)]
	ITO	Sodalime	Magneton sputtering [MTI]	185	8.89	31.3	1.25×10^{21}
	FTO	Sodalime	Spray pyrolysis [Pilkington]	285	12.7	25.1	6.85×10^{20}
	AZO	Sodalime	Magneton sputtering [MSE Supplies]	795	8.77	16.2	5.51×10^{20}
Single crystalline	GaN	Sapphire	HVPE [Kyma]	2,470	73.9	229	1.49×10^{18}
	β-Ga_2O_3 film	Sapphire	LPCVD[28]	12,500	36.5	72.1	1.90×10^{18}
	β-Ga_2O_3 bulk	β-Ga_2O_3	Melt growth [Tamura]	680,000	0.685	71.9	1.86×10^{18}
	SiC bulk	4H SiC	Physical Vapor Transport [II-VI]	352,000	0.469[d)]	150[24]	2.53×10^{18}

[a)]Three separate single layer CVD graphenes were transferred. The graphene sample consists of stacked three single layer graphenes.; [b)]Sheet concentration [#/cm^2] is shown and majority carrier is hole.; [c)]Sheet resistance, mobility, and carrier concentration were estimated from spectroscopic ellipsometry fitting.; [d)]Sheet resistance was measured using a contact-less probe from Semila LEI (PA, USA).

The lifetime laser damage performance of a wide range of transparent conductive materials is assessed, including metals, metal oxides, semiconductors, and graphene whose carrier densities span 5 orders of magnitude from 10^{18} to 10^{23} cm^{-3}. Laser damage threshold measurements with opto-electrical measurements offer systematic criteria to select materials aimed at handling high optical powers in optoelectronics devices and plasmonic metamaterials.

Keywords: Laser damage, transparent conducting films, plasmonics, metamaterials

*Jae-Hyuck Yoo, Andrew Lange, John Chesser, Steve Falabella, and Selim Elhadj**

A Survey of Transparent Conducting Films and Opto-Electrical Materials for High Optical Power Applications